Journal of Applied Sciences

ISSN 1812-5654

science alert

ANSInet
an open access publisher
http://ansinet.com

Journal of Applied Sciences 10 (23): 3141-3155, 2010
ISSN 1812-5654

Semiconductor Detectors and Principles of Radiation-matter Interaction

M. Rizzi, M. D'Aloia and B. Castagnolo
Dipartimento di Elettrotecnica ed Elettronica, Politecnico di Bari, V.E. Orabona, 4-70125 Bari, Italy

Abstract: Semiconductor devices are widely used as radiation detectors in a large variety of fields such as nuclear physics, elementary particle physics, optical, x-ray astronomy, medicine, material testing and so on. As the detector working mode is dependent not only on the adopted material and the chosen architecture, but also on the detection method, the paper reviews the various radiation types, the principles of physics in detection, the semiconductor detector operational characteristics and the semiconductor device structures.

Key words: Semiconductor detectors, radiation-matter interaction, X-ray, heavy charged particles

INTRODUCTION

The success of semiconductor materials as radiation detectors depends on to several characteristic properties that are not available with other detector types. The combination of extremely precise position measurement with high readout speed, the direct availability of signals in electronic form, the simultaneous precise measurement of energy and position and the possibility of integrating detector and readout electronics on a common substrate are some of the obtainable benefits.

In particular, silicon (Si) or germanium (Ge) materials lead to excellent energy resolution but Si is characterized by low stopping power for high energy photons while the small band-gap of Ge makes it able to operate only at cryogenic temperature. Compound semiconductors such as GaAs, CdTe, CdZnTe and HgI_2 have been studied with the aim of realizing high efficiency detectors (Bertuccio, 2005; Rizzi *et al*., 2005, 2006a; Rizzi and Castagnolo, 2003). For a specific application, the selection of the most suitable material among semiconductors depends on the energy range of interest.

Devices realized adopting semiconductor materials exhibit crystal flaws which can be caused by dangling bonds at interfaces or by the presence of impurities in the substrate. The presence of these defect centres, or traps, in semiconductor substrates may significantly influence the device electrical characteristics. Trap centres, whose associated energy lies in the forbidden gap, exchange charges with semiconductor conduction and valence bands through the emission and recombination of electrons. Therefore, trap centres change the space charge density in the semiconductor bulk and consequently, they both influence the recombination statistics and induce distortions in the electric field distribution. Moreover, these defects reduce the detector collection efficiency and the energy resolution (Dubari *et al*., 2002; Cola *et al*., 1996, 1997; Beaumont *et al*., 1992; Rizzi *et al*., 2003, 2004, 2006b).

Therefore, in designing radiation detectors, close attention should be paid to semiconductor growth, device structure and technology processes.

As, both detectors and detection methods are currently field of developments and investigations, this review study considers, also, the physics principles of radiation interaction with matter as a general knowledge background needed to understand how radiation can be detected. Therefore, the second section is dealing with radiation matter interaction taking into account both directly and indirectly ionizing beams.

For the detector performance evaluation, some characteristic parameters are introduced. In fact, energy resolution, detection efficiency and dead time are some of the detector properties presented in the third section.

A particular attention has given to the discussion of semiconductor detectors. In fact, the last three sections are dedicated to review both the effects of radiation interaction in semiconductor materials, the detector working basic principles and the main features of semiconductor detectors. Moreover, the construction methods and the operating characteristics of the most popular semiconductor detectors are briefly described, too.

RADIATION-MATTER INTERACTION

Radiation detector operating mode strongly depends on the mechanisms in which the radiation interacts with the material composing the device.

Corresponding Author: Prof. Maria Rizzi, Dipartimento di Elettrotecnica ed Elettronica, Politecnico di Bari, V.E. Orabona, 4-70125 Bari, Italy Fax: +39 080 5963410

When a radiation beam penetrates the matter, it may be absorbed or scattered or it may pass straight through, without any interaction. The processes of absorption and scattering can be described in terms of interactions between particles; in fact particles of the radiation flux strike particles in the material and are either stopped or scattered. The interaction results in full or partial transfer of incident radiation energy to electrons or nuclei of constituent atoms, or to charged particle products of nuclear reactions.

Radiations can be classified in directly and indirectly ionizing beam. Charged particles (such as fast electrons and heavy charged particles) and uncharged radiations (such as neutrons, X-ray and γ-ray) are examples of the first and the second group, respectively (Jevremovic, 2008).

Charged particle interactions

Heavy charged particles: Heavy charged particles interact with matter primarily through anelastic collisions due to Coulomb forces between their positive charge and the negative charge of orbital electrons belonging to the absorber atoms. The interaction beam energy transferred to the absorbing medium may be sufficient either for raising electron to a higher energetic level (excitation phenomenon) or for removing completely electrons from the atom which they belong to (ionization phenomenon).

Because of the maximum energy that can be transferred from a charged particle to an electron in a single collision is a small fraction of the total incident beam energy, many interactions occur during the travelling of radiation through the matter. Ejected electrons during their motion can produce other ion pairs or secondary electrons. As a consequence of interactions, the charged particle velocity decreases until the particle is stopped.

The amount of energy which is lost by the beam inside the material is measured by the linear stopping power parameter (S) defined as:

$$S = -\frac{dE}{dx} \quad (1)$$

where, dE represents the differential energy loss for the particle under consideration within the material and dx is the differential path length.

The term-dE/dx along a particle track is also indicated as the specific energy loss or the rate of energy loss.

This parameter has been demonstrated to increase as both the number of charge particles increases and high density materials are adopted (Knoll, 2010).

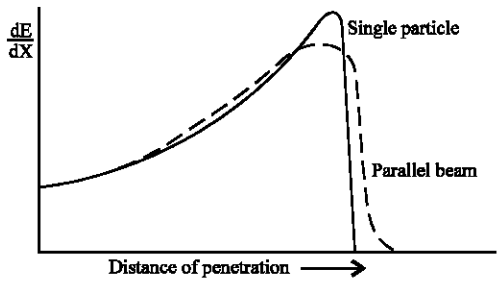

Fig. 1: The bragg curve along an alpha ray track

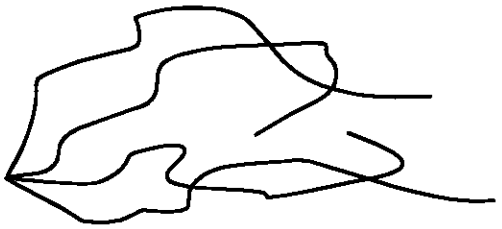

Fig. 2: Fast electron path along absorbing material

The plot of the specific energy loss along the charged particle track is known as the Bragg curve (Fig. 1). As it is shown, there is a pronounced peak in the curve plot immediately before the particles come to rest. A peak occurs because the interaction cross section increases as the charged particle energy decreases (Jakubek *et al*., 2008).

Fast electron interactions: Fast electrons move inside the absorbing material with a tortuous path and because of their mass is equal to that of orbital electrons, a large amount of energy can be lost in a single interaction (Fig. 2).

Moreover, for this type of particles, energy may be lost by radioactive processes as well as by coulomb interactions. For beta particles having typical energy of about a few MeVs, radioactive losses are small in comparison with ionization and excitation losses if the absorber material has a small atomic number value.

Due to the electron track deflections, backscattering phenomenon may take place. For this reason, electrons entering the detector surface can re-emerge from the same surface and consequently they do not deposit all their energy inside the material. Therefore, backscattered electrons have a great influence on the detector designed to evaluate the energy of interacting electrons (Hoheisel *et al*., 2005).

Uncharged radiations

Gamma an X-ray interaction: Unlike charged particles, uncharged radiations do not steadily lose energy as they

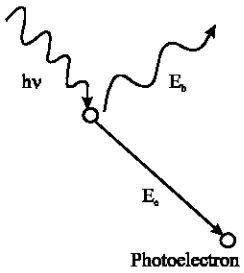

Fig. 3: The photoelectric effect of an incident photon

penetrate matter. Instead, they can travel some distance before interacting with an atom.

Different situations may occur when a photon interacts with materials. In fact, it might be absorbed and consequently, it disappears or it might be scattered, changing its direction of travel, with or without loss of energy.

Many mechanisms can take place when γ and X-rays hit matter; for example Thomson and Rayleigh scattering are two processes by which photons interact with matter without appreciable transfer of energy. But the most important interaction mechanisms are the photo electric effect, the compton scattering and the production of pairs which are characterized by photon energy deposition in matter.

In the photoelectric effect, the interacting photon is completely absorbed by the atom and an energetic photoelectron is ejected by the same atom from one of its bound shell (Fig. 3). The photoelectron appears with the following energy E_e:

$$Ee = h\nu - E_b \quad (2)$$

where, E_b is the photoelectron energy in its original shell (the binding energy) and hν the ray energy.

As consequence of the emission, an ionized atom with a vacancy is created, too. This vacancy is filled by a free electron of the absorber medium or by an electron belonging to other shells of the same atom. Therefore, X-ray photons or Auger electrons are generated.

The photoelectric effect is the predominant interaction mechanism both for γ and X-ray of low energy and for material of high atomic number (Z). In fact the photoelectric absorption probability is proportional to Z^n with n varying between 4 and 5.

When, the compton scattering process takes place, the incident beam interacts with a material electron (indicated as recoil electron) transferring to it some of its energy and it is deflected of an angle θ with respect to its original direction (Fig. 4). The scattered radiation wavelength (λ') is linked both to the wavelength incident

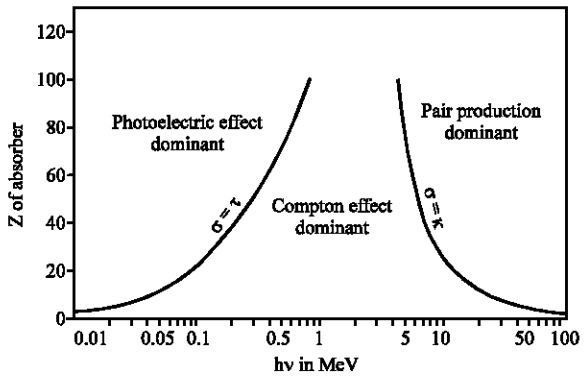

Fig. 4: Compton scattering of an incident photon

beam (λ) and to the deflected angle according to the following expression:

$$\Delta\lambda = \lambda' - \lambda = \lambda_e(1 - \cos\theta) \quad (3)$$

where, Δλ is the wavelength Compton shift and λ_e is the Compton wavelength of the electron.

It is evident that Δλ grows as the scattering angle increases and it reaches the maximum value for θ = π.

The energy transferred from the incident beam to the electron can varies from zero to a large fraction of the incident ray energy, according to the following relation:

$$h\nu' = \frac{h\nu}{[1 + \Delta(1 - \cos\theta)]} \quad (4)$$

with $\Delta = h\nu/mc^2$ representing the reduced energy of the incoming photon and mc^2 the rest mass energy of the electron.

When, the ray energy exceeds twice the electron rest mass energy (i.e., $2\ mc^2 \approx 1.02$ MeV), the phenomenon of electron and positron pair production is possible in the field of an atomic nucleus. It can also occur in the field of an atomic electron but with a lower probability, being necessary a ray energy quadruple of the electron rest mass energy (this process is named triplet production as the presence of recoil atomic electron over electron-positron pair).

The photon energy (hν) is completely absorbed and is converted into $2\ mc^2$ plus the kinetic energy of the electron and the positron. The inverse process occurs when an electron and a positron annihilate and they produce photons.

The effect of the previous three mechanisms in relation with material atomic number and incident ray energy is reported in Fig. 5. It is evident that the Compton effect dominates at medium Δ and low Z-values. At high

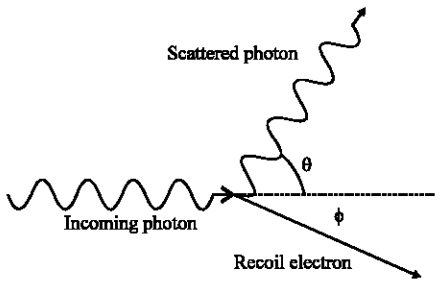

Fig. 5: The effect of the three major radiation matter interaction phenomena in function of Z and hν

Δ and high Z, the pair production mechanism is the relevant process of photon interaction in matter. At low Z and low Δ, the photoelectric process becomes the dominant process of photon interaction.

Each of X or γ-ray interaction processes previously described, can be characterized by a probability of occurrence per unit path length in the absorber. The sum of these probabilities represents the probability per unit path length that the ray photon is removed from the beam. This probability, denoted by ì and having dimension of an inverse length, is called the linear attenuation coefficient (or macroscopic cross section). The coefficient μ depends on both the photon energy and the material which is traversed; it is expressed as follows:

$$\mu = \tau+\sigma+\kappa \quad (5)$$

where, τ, σ and κ are the probability of photoelectric, Compton and pair interaction occurrence, respectively.

Therefore, a collimated X or γ-ray of initial intensity I_0, after traversing a material with thickness x will have a residual intensity of unaffected primary photons I (photons that do not interact) equal to:

$$I = I_0 e^{-\mu x} \quad (6)$$

The quantity μ^{-1}, indicated with λ, is the mean free path (or mean path length) that represents the average distance traveled by the ray inside the absorber before an interaction takes place.

As the coefficient μ is dependent on the material density, a more convenient figure is introduced (named mass attenuation coefficient) which is defined as μ/ρ with ρ denoting the medium density (Yaffe and Rowlands, 1997).

Neutron interaction: Like photons, neutrons are uncharged particles and therefore do not interact with matter by means of coulomb force. They can travel appreciable distances inside matter without interacting but when they interact it is with a nucleus of the absorbing material.

The secondary radiations resulting from neutron interaction are almost always heavy charged particles. They may be produced either as result of nuclear reactions or they may be the nuclei of the absorbing material which have increased their energy as result of neutron collisions. In fact, a neutron can collide with an atomic nucleus, which can scatter it elastically or inelastically. The scattering type is elastic when the energy lost by the neutron is equal to the kinetic energy of the recoil nucleus (i.e., the total kinetic energy is conserved) while it is inelastic when the nucleus absorbs some energy and remains in an excited state.

The neutron can also be captured, or absorbed, by a nucleus, leading to a reaction, such as (n, p), (n, 2n), (n, α), or (n, γ).

The probability of different neutron interaction occurrence depends on neutron energy.

RADIATION DETECTOR PROPERTIES

In a wide category of detectors, when a particle or a radiation quantum interacts with material according to one of the previous discussed mechanisms, the net result is the appearance of an amount of electric charge inside the detector active volume. Applying an electrical field within the detector, a flow of charges is originated. The time required for the charge collection is related to the particular detector, in fact it depends on the charge carrier mobility and on the average distance that must be travelled before arrival at the collecting electrodes. Therefore, the response of a detector to a single particle or to an interacting quantum of radiation is a current that flows for a time equal to the charge collection time. Obviously, the time integral over the current duration is the charge generated during the interaction process.

In this analysis a low interaction rate is considered, so that each individual interaction gives rise to a current that is distinguishable from the others. In real situation, current flows in the detector from more than one interaction at a given time.

Detector working modes: Three different detector working modes can be considered: pulse mode, current mode and mean square voltage mode.

If the response time of the measuring device connected across the detector output terminals is long compared with the average time spacing between current pulses, then a current is recorded that is given by the mean rate of charge formation averaged over many

individual radiation quanta. This mode of operation is called current mode. The average current represents the product of the average event rate and the charge created per event. However, different currents will result from radiations that have equal interaction rates but deposit a different average energy per interaction.

In mixed radiation environments, when the charge amount produced by various radiation types is different, detectors operating in mean square voltage mode are useful. In such devices, the mean square of the time variance of the detector current is recorded which is proportional to the event rate and the square of the charge produced in each event.

In the pulse mode operation, each quantum of radiation that interacts with the detector has to be measured. The output of such type of detector is a sequence of individual signal pulses, each representing the result of a single quantum of radiation within the detector. The rate at which such pulses occur, give a measure of the radiation interactions inside the detector while the amplitude of each pulse is related to the amount of charge generated during each interaction.

Pulse mode operation is the most common choice for different radiation detector applications; in fact it presents several advantages (for instance a higher sensitivity) in comparison with the other two working modes.

Pulse height spectra and energy resolution: In the pulse mode detector, the amplitude of the various pulses is different because of differences in radiation energy or fluctuations in detector response to a monoenergetic radiation. The pulse amplitude distribution gives information about the incident radiation. In Fig. 6 an example of the differential pulse height distribution is indicated: the value of dN/dH is plotted vs. the pulse amplitude where dN is the differential number of pulses with an amplitude within the differential increment dH. The number of pulses having an amplitude between H_a e H_b is obtained adopting the following expression:

$$\int_{H_a}^{H_b} \frac{dN}{dH} dH \tag{7}$$

In many applications, the radiation detector task is the energy distribution measure of the incident radiation. The capability of detectors to distinguish between two particles or photons with different but close energies is indicated as the energy resolution and denoted with R.

A large amount of fluctuations in the number of produced charges is recorded even if radiation beams with equal energy are adopted. There is a high number of potential sources of fluctuations in the response of a

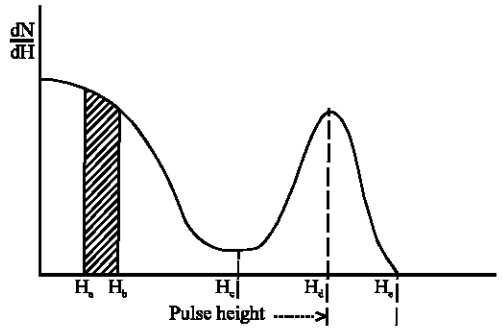

Fig. 6: Differential pulse height distribution plot

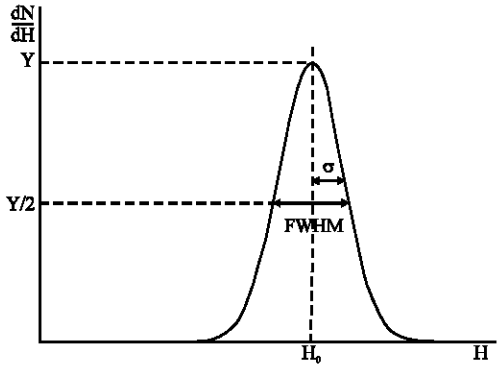

Fig. 7: Parameter identification for the energy resolution definition

detector that result in imperfect energy resolution. They can be produced by drift of the detector operating characteristics, random noise sources of the instrumentation system and statistical noise derived from the fact that the charge generated within the detector by a radiation quantum is not a continuous variable but represents a discrete number of charge carriers.

The energy resolution is defined as the Full Width at Half Maximum (FWHM) divided by the location of the peak centroid H_0, having indicated with FWHM the width of the distribution at a level that is half the maximum ordinate of the peak (Fig. 7). It is evident that the smaller the value of R, the better the detector will able to distinguish between radiations having energies lie near each other. Assuming that the formation of each charge carrier is a poisson process, it was demonstrated that for detector having a linear response, R results (Knoll, 2010):

$$R = \frac{2.35}{\sqrt{N}} \tag{8}$$

where, N is the average number of generated charge carriers.

For some type of detectors, experimental results show that the obtained R-values are lower than the values predicted by Eq. 8. This difference indicates that the processes which give rise to the generation of charge carriers are not independent and therefore the total charge produced cannot described by a simple poisson process. A corrective parameter, called the Fano factor and indicated with F, is introduced to quantify the difference of the observed values from the number of charge carriers obtained considering a pure Poisson statistic (Fano, 1947). Introducing the Fano factor, expression Eq. 8 becomes:

$$R = 2.35\sqrt{\frac{F}{N}} \quad (9)$$

Detection efficiency: Charged radiation interacts with detector producing ionization or excitation of material nuclei as it enters in the active volume. Therefore, after a typical particle is travelled a small fraction of its range, a lot of pairs is created to ensure the presence of a signal pulse large enough to be detected. In this situation no charged particles reaching the detector active volume are lost. The detector has a 100% detection efficiency.

On the contrary, uncharged radiations can travel some distance before interacting with a material atom; therefore detector have, generally, an efficiency value less than 100%.

In order to relate the number of counted pulses to the number of hitting photons, the absolute (ε_{abs}) and the intrinsic (ε_{int}) efficiency are evaluated with the following expression:

$$\varepsilon_{abs} = \frac{\text{Number of pulses recorded}}{\text{Number of quanta generated by source}} \quad (10)$$

$$\varepsilon_{int} = \frac{\text{Number of pulses recorded}}{\text{Number of quanta hitting the detector}} \quad (11)$$

The intrinsic efficiency, which is the most used parameter, depends on the detector material, the radiation energy, the detector thickness in the direction of incident radiation. Moreover, a slight dependence on the distance between the source and the absorber material is observed as the average path length of the ray inside the detector changes somewhat with this spacing.

Dead time: The dead time is the time during which a detector is not able to detect a next coming particle, in fact two events must have a minimum amount of separation in time in order to be recorded as two different pulses. This minimum recording time can be determined by physical processes in the detector or by associated electronics. For example, when a radioactive sample is counted, the possibility can arise that two interactions in the detector will occur too close together in time to be registered as separate events.

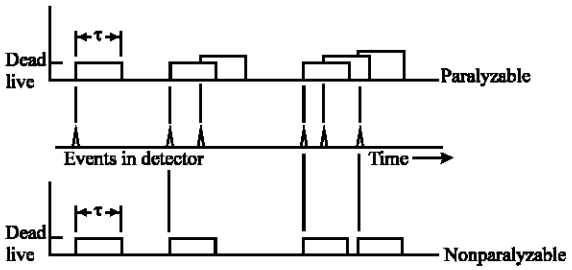

Fig. 8: Fundamental assumptions of the two different models for detector dead time behaviour

Two different models have been proposed to approximate the dead time behaviour of counting systems: paralyzable and nonparalyzable response.

A paralyzable detector is unable to provide a second response until a certain dead time τ has passed without another event occurring. Another event during τ causes the insensitive period to be restarted.

A nonparalyzable detector, on the other hand, simply ignores other events if they occur during τ.

Differences in the two models are illustrated in Fig. 8. The central line represents six events as they occur along the horizontal time axis, and the other two axes show the responses of the two types of detectors. Of the six events in this example, the paralyzable counter registers three and the nonparalyzable, four.

Denoting with r_i and r_c the true interaction rate and the recorded count rate respectively, the fraction of time that the nonparalizable detector is dead is $r_c \tau$. Therefore, the fraction of time that it is sensitive is $1-r_c \tau$, which is also the fraction of the number of true events that can be recorded as it is expressed in the following formula:

$$\frac{r_c}{r_i} = 1 - r_c\tau \quad \text{(nonparalizable model)} \quad (12)$$

In the paralyzable case, dead periods are not always of fixed length. The average number of events that takes place in a time t is $r_i t$. If an event occurs at time t = 0, then the probability that no events occur in time t immediately following that event is given by the Poisson term, with P_0 expressed as:

$$P_0 = e^{-r_i t} \quad (13)$$

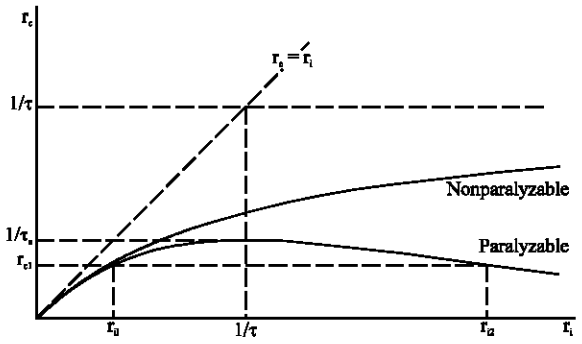

Fig. 9: Plot of the observed rate vs. the true rate for nonparalyzable and paralyzable models

Therefore, given an event at time t = 0, the probability that the next event will occur between t and t + dt is:

$$P(t)dt = re^{-r_i t}\,dt \tag{14}$$

The probability that a time interval larger than τ will elapse is:

$$\int_{\tau}^{\infty} r_i e^{-r_i t} dt = e^{-r_i \tau} \tag{15}$$

The observed count rate r_c is:

$$r_c = r_i e^{r_i \tau} \quad \text{(paralyzable model)} \tag{16}$$

For low event rates or short dead time ($r_i\tau < 1$), the two models lead the same results:

$$r_c = \frac{r_i}{1 + r_i \tau} \approx r_i(1 - r_i \tau) \qquad \text{(nonparalizable model)} \tag{17}$$

$$r_c = r_i e^{-r_i \tau} \approx r_i(1 - r_i \tau) \qquad \text{(paralyzable model)} \tag{18}$$

Plotting r_c vs. r_i it is evident that for nonparalyzable model r_c cannot exceed τ^1, which is an asymptotic value, while for paralyzable model r_c reaches a maximum value equal to $e\tau^{-1}$ (Fig. 9). Increasing the event rate, the measured count rate with a paralyzable system will decrease beyond this maximum and will approach zero, because of the decreasing opportunity to recover between events. With a paralyzable system, there are generally two possible event rates that correspond to a given count rate.

SEMICONDUCTOR DETECTORS

Radiation detection system is composed of a detector, signal processor electronics and data output display device such as counter or multichannel analyzer. Detector physical properties and characteristics control detection system features.

Radiation detectors and detection systems can be classified differently according to the particular parameter taken into account. In fact, they can distinguish into.

- Gas, liquid and solid if the detector physical form is considered
- Current (ions) and light if the nature of the detector output signal is observed
- Counting, pulse height spectrometry, dosimetry, imaging and timing if their function is pointed out

It is very clear that there are many varieties of detection systems.

Devices employing semiconductors as detection medium have become very diffused in many radiation detection applications. The information carriers are electron/hole pairs which are generated along the path taken by the charged particle through the detector. The large number of generated carriers for a given incident radiation beam, produces detectors with good energy resolution. Moreover, other features can be obtained adopting semiconductor as absorber material such as compact sizes and relatively fast timing characteristics.

Semiconductor properties: The periodic structure of the particular crystalline material establishes allowed energy bands for electrons which are present inside the material. The lower band, indicated with valence band, is composed of electrons which are bounded to lattice sites inside the crystal while the upper band, denoted with conduction band, is characterized by the presence of free electrons which contribute to the material conductivity. These two bands are separated by a band of forbidden states named bandgap. The bandgap dimension defines the classification of material as conductor, semiconductor or insulator.

In absence of thermal excitation, semiconductor exhibits a valence band fill of electrons while a conduction band totally empty. If an energy exceeding the bangap energy is imparted to an electron located in the valence band, this electron can be transferred to the conduction band and a vacancy (called hole) is created inside the valence band. The average displacement of a movable charge carrier due to random motion is zero but owing to the application of an electrical field, both the electron within the conduction band than the hole inside the valence band (which represents a positive charge) can move contributing to the material conductivity. Because of electrons is drawn in a direction opposite to the electric field, holes move in the same direction as the electric field with the following net drift velocity:

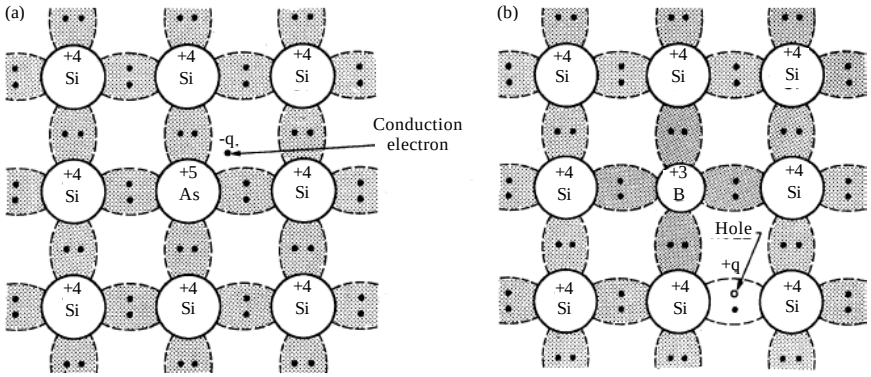

Fig. 10: Bond representation for (a) n type and (b) p type semiconductor

$$v_n = \mu_n E \quad (19)$$

$$v_p = \mu_p E \quad (20)$$

where, v_n and v_p represent the drift velocity of electrons and holes, respectively, μ_n and μ_p the semiconductor electron and hole mobility, E the electrical field magnitude

Relations Eq. 19 and 20 are valid for electrical field magnitudes small enough so to produce carrier velocity change which is small in comparison with the thermal velocity. Alternatively, if the field is high enough, such that electron and hole energies become appreciably larger than the thermal energies, strong deviations from linearity are observed and drift velocities become independent of the electric field, reaching a saturation value.

An other way to obtain free electrons is the alteration of semiconductor lattice structure adding a small amount of other elements with a different atomic structure (called impurities). This procedure, which can be performed either during crystal growth or later in selected crystal regions, is called doping. In this way, the electrical properties of pure semiconductor materials can be modified and controlled.

When, impurity elements, also called dopants, are added to semiconductor material, impurity atoms take the place of semiconductor atoms in the lattice structure. When impurity atoms have one more valence electron than the semiconductor atom, this extra electron cannot form an electron pair bond because no adjacent valence electron is available and it requires only slight excitation to break away. Consequently, the presence of such excess electrons increases the semiconductor conductivity. The resulting material is called n-type because the excess free electrons have a negative charge and the impurities of this type are referred to as donor atoms. In this case, electrons are called majority carriers and holes minority carriers.

A different effect is produced when impurity atoms having one less valence electron than the semiconductor atom is substituted in the lattice structure. Although all the valence electrons of the impurity atoms form electron pair bonds with electrons of neighbouring semiconductor atoms, one of the bonds in the lattice structure cannot be completed because the impurity atom lacks the final valence electron. As a result, a vacancy (hole) exists in the lattice and an electron from an adjacent electron pair bond may absorb enough energy to break its bond and to fill the hole. As in the case of excess electrons, the presence of holes encourages the flow of electrons in the semiconductor material with a consequently increasing of the material conductivity. Semiconductor of this type having an excess of holes is called p-type material and the adopted impurities are indicated as acceptor atoms (Fig. 10) (Millman and Grabel, 1988).

Radiation interaction in semiconductor: Radiation interaction with semiconductor materials produces the creation of electron-hole pairs that can be detected as electric signal. As it is shown in the previous sections, when the incident ray is composed of charged particles, ionization may occur along the path of flight by many collisions with the electrons. In presence of uncharged radiations, such as X-ray, photons have first to undergo an interaction with either a target electron (according to photoelectric or compton effect) or with the semiconductor nucleus.

The average energy converted into electron/hole pair creation, called ionization energy and indicated with ε, is specific of the particular absorbing material. Moreover, it is weakly depended on the type and energy of the incident radiation except for low energies which are comparable with the semiconductor band gap. This characteristic allows interpretation of the number of electron/hole pairs produced in terms of the radiation incident energy, provided the particle is fully stopped inside the detector active volume. The ε-value for silicon and germanium is about 3eV, lower than the typical value

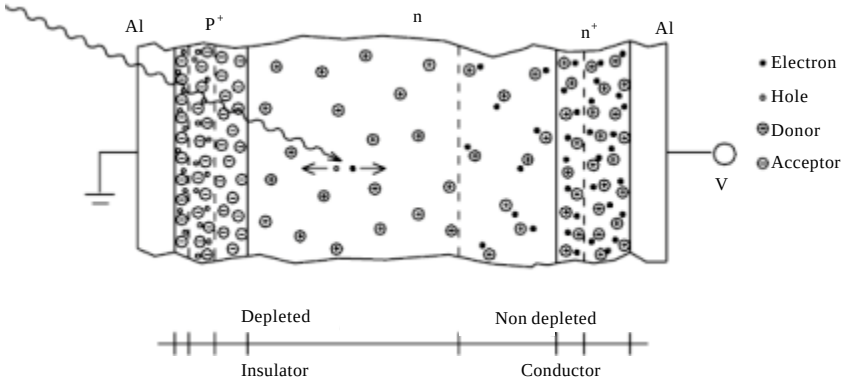

Fig. 11: Example of a p-n junction diode

of gas detector; consequently, for an absorbed energy E, an increased number of charge carriers is produced in Si or Ge detectors. The mean number of generated pairs N is obtained with the following expression:

$$N = \frac{E}{\varepsilon} \quad (21)$$

The fluctuation in the number of carriers generated can be evaluated introducing the Fano factor F:

$$\text{Variance in pair number} = FN \quad (22)$$

After the electron/hole generation inside the semiconductor, the created charges will tend to migrate either spontaneously or for an electrical field application. Their motion will go on until they are collected at the electrodes or they recombine because of the presence of impurities or structural imperfections of the detector material. Recombination produces an incomplete charge collection. In particular, impurities inside the semiconductor act as traps because they introduce additional energy levels inside the forbidden gap (deep impurities). These levels could capture electrons or holes and they release them after a time period. Obviously, if the trapping time is long, the captured carriers cannot contribute to the measured pulse.

Some other deep impurities can act as recombination centres. These impurities are able to capture all the type of carriers. In fact, they could capture first an electron from the conduction band and then a hole coming from the valence band with the result of carrier annihilation.

Also structural defects within the crystal structure of the semiconductor can lead to trapping phenomenon and charge carrier loss (Ponpon, 2005).

Semiconductor junction: The usefulness of semiconductors as electronic circuit elements and for radiation measurements stems from the special properties obtained when n and p type semiconductors are brought into good thermodynamic contact creating a diode junction. In practice, such a junction is built by diffusing acceptor impurities into a n type silicon crystal or by diffusing donor atoms into a p type silicon crystal. An example of p-n junction detector is shown in Fig. 11. It consists of a highly doped shallow p^+ region on a very lowly doped n-substrate, the back portion of a highly doped n^+ layer. The n^+ layer provides a good ohmic contact from the aluminium to the substrate and simultaneously it allows operation of the device in overdepleted mode.

A charge depleted region occurs at the interface of the n and p type regions. This depleted region is created as the result of both electron diffusion from n type material into p type and hole diffusion from p type to n type material. Therefore, diffusion is responsible for the existence of a space charge region composed of two zones: a first zone made of filled electron acceptor sites not compensated by holes and a second zone made of positively charged empty donor sites not compensated by electrons.

The space charge creates an electrical field that reduces the tendency for further diffusion. At equilibrium the field is adequate to prevent additional net diffusion across the junction and a steady state charge distribution is therefore established.

Therefore, the depletion region acts like a high resistivity parallel plate ionization chamber, making it feasible to use diode junction for radiation detection. Due to the electric field presence, electron/hole pairs produced within the depleted region migrate out and their motion gives rise to an electrical signal. For this reason, the depletion region represents the sensitive volume of the semiconductor detector.

Unbiased p-n junction can act like a detector but only with very poor performance because both the depletion

region thickness is small, the junction capacitance is high and the electric field strength across the junction is low and not enough to collect the induced charge carriers that, consequently, could be lost due to trapping and recombination.

The performance of the p-n junction as a practically used radiation detector is improved by applying an external voltage that leads the junction to be reversed biased. As the applied voltage raises, both the width of the depletion region (i.e., the sensitive volume) increases, the junction capacitance decreases and the detection performance improves (Millman and Grabel, 1988).

Semiconductor detectors can operate with a reverse bias voltage that can produce either a space charge region contained within the interior volume of the wafer (partially depleted detector) or a space charge region that extends through the full wafer thickness (fully depleted detector).

However, the applied voltage should be kept below the breakdown voltage of the detector so to avoid a catastrophic deterioration of detector properties.

Charge transport in semiconductor junctions: The motion of charge carriers generated by an ionizing particle in a semiconductor detector produces a signal with a shape which is determined by the detector charge transport properties. Diode charge transport properties depend on Millman and Grabel (1988):

- The dopant effective concentration (N_{eff}), which defines the internal electric field and thus, the depletion voltage value
- The electron (μ_e) and hole (μ_p) mobilities, which influence the time needed to collect the charges
- The charge trapping lifetime for hole and electron (τ_{tp}, τ_{te}), which affect the charge collection efficiency

First, let us assume a simplified model where the electron and hole mobilities are constant with the electric field.

Ramo's theorem relates the displacement (Δx) of a charge carrier q generated by the passage of an incoming particle in the detector to the charge (ΔQ) collected on the electrodes:

$$\Delta Q = q\frac{\Delta x}{w} \tag{23}$$

with w denoting the electrode distance.

The induced current is:

$$i(x) = \frac{dQ}{dt} = \frac{q}{w}\frac{dx}{dt} = \frac{q}{w}v(t) \tag{24}$$

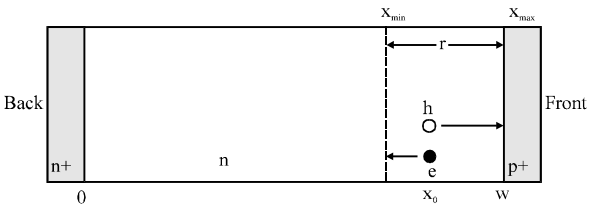

Fig. 12: Motion of an electron/hole pair generated inside the active volume of a p-n junction for the electric field application

Therefore, the induced currents due to electrons ($i_e(x)$) and holes ($i_p(x)$) is, respectively:

$$i_e(x) = \frac{q}{w}\mu_e E(x) \tag{25}$$

$$i_p(x) = \frac{q}{w}\mu_p E(x) \tag{26}$$

where, E(x) is the electric field inside the detector depleted region.

Considering an electron/hole pair generated at $x = x_0$ inside the detector depleted zone and supposing that the applied electric field drifts electrons toward the electrode at x = w while holes in the opposite direction toward the electrode at x = 0 (Fig. 12). It is easy to demonstrate that with the previous assumptions, the total collected charge Q_{tot} is (Leroy and Rancoita, 2009):

$$Q_{tot} = Q_e + Q_p \tag{27}$$

where, Q_e e Q_p represent the total electron and hole collected charge, respectively. Their values can be evaluated with the following expressions:

$$Q_e = \frac{q}{w}(w - x_0) \tag{28}$$

$$Q_p = \frac{q}{w}x_0 \tag{29}$$

A more accurate analysis is obtained considering the mobility parameters dependent on both the electric field and the temperature and taking into account the generation/recombination phenomena, too. In this situation the Poisson equation and the continuity equations for electrons and holes have to be solved (Leroy *et al.*, 1999):

$$\begin{aligned}
\nabla\psi &= -\frac{q}{\varepsilon}(-N_{eff} - n + p - n_t + p_t)\\
\frac{\partial n}{\partial t} &= -\frac{\partial n_t}{\partial t} + \frac{\nabla J_n}{q} + G - R_n - U_{SRH}\\
\frac{\partial p}{\partial t} &= -\frac{\partial p_t}{\partial t} - \frac{\nabla J_p}{q} + G - R_p - U_{SRH}\\
\frac{\partial n_t}{\partial t} &= \frac{n}{\tau_{te}} - \frac{n_t}{\tau_{de}} - R_{nt}\\
\frac{\partial p_t}{\partial t} &= \frac{p}{\tau_{tp}} - \frac{p_t}{\tau_{dp}} - R_{Pt}
\end{aligned} \quad (30)$$

Where:

G = The electron/hole generation rate
$R_{n(p)}$ = The electron (hole) recombination rate
$\tau_{te(tp)}$ = The electron (hole) trapping lifetime
$\tau_{de(dp)}$ = The electron (hole) detrapping lifetime
n_t (p_t) = The trapped electron (hole) density
J_n (J_p) = The electron (hole) current density
U_{SRH} = The shockley read hall generation-recombination term

SEMICONDUCTOR DETECTOR OPERATIONAL CHARACTERISTICS

Effect of bias voltage on detector performance: In order to produce an electric field large enough to achieve a charge carrier efficient collection, a reverse bias voltage of hundreds or thousands of volts has to be applied between the semiconductor detector electrodes. In fact, if low bias voltage is imposed, the pulse height deriving from radiations that are fully stopped within the depletion region rises with the applied voltage. This variation is due to an incomplete carrier charge collection as consequence of trapping/recombination mechanisms along the incident particle track. The fraction escaping collection, decreases as the electric field is increased.

When a reverse voltage is applied to a junction detector, a current of the order of a fraction of microampere or nanoampere is usually observed (depending on the particular semiconductor material adopted) even in absence of ionizing radiation. The origin of this leakage current are related both to the bulk volume and surface of the detector.

Sources of the bulk leakage current are both the minority carriers, that are conducted across the junction because of the reverse voltage applied, and the thermal generation of electron/hole pairs within the depletion region. The first contribute is generally small while the second depends on the operation temperature. For example, silicon and gallium arsenide detectors have a sufficient low thermally generated leakage current to allow their use at room temperature while germanium devices must operate at reduced temperature as consequence of the lower energy gap.

Surface leakage current takes place at the junction edges where voltage gradients are present. It depends on various factors such as humidity and detector surface contamination.

Random fluctuations that occur in leakage current could tend to obscure the small signal current that flows following an ionizing event and could represent a noise source in many situations. Methods for leakage current reduction, such as guard-rings, have to be taken into account in semiconductor detector design phase.

Pulse rise time: Semiconductor detector timing properties can be evaluated taking into account the output signal rise time. It is composed of the charge transit time and the plasma time contributes.

The charge transit time is related to the motion of electron/hole pairs created by a radiation beam hitting the detector depletion region. Therefore, it depends on the electric field intensity and the spatial charge zone width. In fully depleted detectors, the semiconductor physical thickness fixes the depletion width and consequently, the electric field growth reduces the rise time. In partially depleted detectors, the spatial charge region increases with increasing the applied voltage and therefore the effect of a high voltage bias is to increase both the electric field and the distance over which charge pairs must be collected.

The relation of the charge transit time on the applied bias voltage is enough complicated even if it can be simplified if suitable assumptions are made (Ahmed, 2007).

When, the incident radiation is composed of heavy charged particles, the plasma time component is observed. In fact, in this situation the electron/hole pair density along the track of the hitting particles is sufficient high to form a plasma (like charge cloud) that shields the interior from the electric field influence. Only the charge carriers at the outer edge of the cloud migrate because they are under the influence of the electric field. The outer regions are gradually eroded away till the inner charges are subjected to the applied electric field and they drift. Therefore, the plasma time can be defined as the time required for the charge cloud to disperse to the point where normal charge collection proceeds (Dearnaley, 1966).

Dead layer and channelling: When semiconductor detectors are irradiated with weakly penetrating particles, such as heavy charged particles, an high amount of energy can be lost before the ray reaches the detector active volume. The thickness of this dead layer is, generally, a function of the applied voltage.

When the hitting ray is perpendicular to the detector surface (i.e., the incidence angle is zero), the energy loss in the dead layer is:

$$\Delta E(0) = \frac{dE(0)}{dx} d \quad (31)$$

where, d is the dead layer thickness.

The energy loss for a generic β incidence angle is:

$$\Delta E(\beta) = \frac{\Delta E(0)}{\cos\beta} \quad (32)$$

Moreover, in crystalline materials the energy loss rate of charged particles depends on their path orientation; in fact particles travelling parallel to detector crystal planes are characterized by an energy loss rate lower that that of particles directed in arbitrary directions. These particles (sometimes called channelled particles) penetrate significantly farther through the crystal.

Radiation damage: The radiation process produces inside the detector some damages whose nature depends on the particular particle hitting the semiconductor material. The radiation induced damages can be classified in two categories: bulk and surface type.

The impinging radiation can interact with semiconductor material nuclei producing an irreversible damage. In this situation, a bulk damage is produced (called Frenkel defect) because a material atom is displaced from its normal lattice site. The generated vacancy and the original atom, now at an interstitial position, act as:

- Recombination/generation centres because they are able both to capture and to emit electrons and holes. This alternate emission of electrons and holes inside the detector depleted region increases the leakage current
- Trapping centres because electrons and holes are captured and re-emitted. The trapped signal charge could be released too late producing an incomplete charge collection at the detector electrodes

Moreover, they could change the charge density in the depleted zone and consequently, an increased bias voltage is required to make the detector fully sensitive

Therefore, when enough of these defects are generated, carrier lifetime and charge collection efficiency are reduced while detector energy resolution is degraded because of fluctuations in the charge lost amount.

After the end of the irradiation process, it is possible to notice that the produced damage to the detector reduces with time. This effect is called annealing. The rate of damage decrease is strongly dependent on the temperature at which the detector is kept during the waiting period. True annealing, in which the crystal becomes perfect again, does exist but in many cases defects may just be transformed into other more stable defect types with changed properties.

Surface damages involve charge build up either at interface or in overlaying electrically insulating layers (i.e., a thermal oxide on silicon) and can cause heavy surface inversion or accumulation. In fact, energy absorbed by electronic ionization in insulating layers liberates charge carriers which diffuse or drift to other locations where they are trapped, leading to unintended concentrations of charge and as a consequence, parasitic fields.

Therefore, oxide damage is caused by ionizing irradiation such as photons, x-rays and charged particles, while semiconductor bulk damage, requiring damage of the crystal structure, is generated by massive particles such as neutrons and protons (Janesick *et al*., 1989; Kim *et al*., 1995; Lutz, 2007).

SEMICONDUCTOR DETECTOR CLASSIFICATION

Existing semiconductor detectors differ from one another because of the adopted material or the method by which the material is treated.

In the following sections, construction methods and operating characteristics of the most popular semiconductor detectors are briefly described (Tsoulfanidis, 1995; Akimov, 2007).

Surface barrier detectors: A p-n junction is created on a n type semiconductor by evaporation of a thin gold layer which acts as an acceptor and simultaneous serves as an electrode. Best results are obtained if the evaporation phase is carried out under conditions that produce surface oxidation. In fact, as a result of surface oxidization, surface energy states are produced that induce a hole high density so to form a p type layer on the surface. Moreover, the oxidation layer reduces the surface leakage current improving the detector performance.

Hence, the front electrode operates as a rectifying contact, while the back electrode serves only as an ohmic contact.

Diffused and implanted junction detectors: A homogeneous crystal of p-type material is the basic material for this detector types.

One surface of the wafer is doped by diffusing n type impurities at high temperature (typically phosphorus) so to create a thin n type semiconductor layer. Therefore, a p-n junction is formed which has a depleted zone extended primarily into the semiconductor p type zone as the n type surface layer is heavily doped compared with

the p type crystal. For the reasons previously described, much of the surface layer is outside the depletion region and it represents a dead layer. In some applications, the dead layer presence is a disadvantage as an amount of particle energy is lost before the detector active zone is reached.

An alternative method to introduce doping impurities at semiconductor surface is the ion implantation method which makes the concentration profile of the added impurity controllable by changing the incident ion energy. To reduce the radiation damage caused by the incident ions, a subsequent annealing step is necessary which is characterized by a process temperature lower than the one which is needed for the diffusion of dopants to form a diffused junction. For this reason, a reduced defect number is produced and consequently, a lower leakage current is expected in comparison with diffused barriers.

Lithium drifted junction detectors: Using conventional junction techniques it is not possible obtaining very wide depletion layers. To provide detectors of greater sensitive volume, a process has been devised which creates a region of compensated or intrinsic semiconductor in which donor and acceptor concentration are balanced. These detectors are called lithium drifted silicon detector or lithium drifted germanium detector and designed as Si(Li) or Ge(Li).

During the fabrication process, lithium is diffused through one surface of a p type crystal where it acts as a donor impurity. The resulting p-n junction is reverse biased while the crystal temperature is increased to enhance the mobility of lithium donors. Lithium donors are slowly drawn by the electric field into the p type semiconductor where their concentration will increase and approach that of the original acceptor impurities. Thus, a region is created that looks like an intrinsic semiconductor (Bertolini and Coche, 1968; Pell, 1960; Gibbons and Iredale, 1967; Lauber, 1969).

Once the drifting process is completed, the detector has the configuration indicated in Fig. 13.

The process of compensating impurities by drifting lithium into a semiconductor, has been developed to produce either silicon and germanium devices.

More recently, detectors having wide active volume are possible adopting the high purity germanium configuration (HPGe) and consequently, Ge(Li) is no longer popular. However the technique remains important in silicon.

Compound semiconductor detectors: Besides semiconductors composed of a single chemical element (such as Si and Ge), various semiconductors exist in

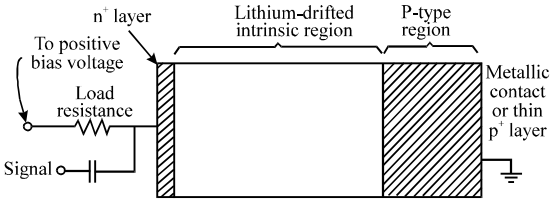

Fig. 13: Lithium drifted junction detector configuration

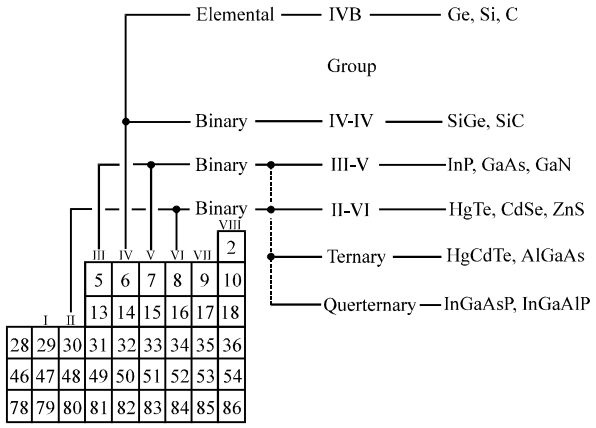

Fig. 14: Compound semiconductor list

which atoms of a different element are able to substitute a particular material without altering its crystal structure. A list of this materials, called compound semiconductors, is shown in Fig. 14 where, the main group and their composing elements are indicated.

In particular, compound semiconductors have many advantages arising from wide range of stopping powers to band gaps available. Mixing and matching available band gaps and stopping powers appropriately, different radiation detectors for specific applications can be realized. For example, an energy gap closed to 1.5eV, minimizes leakage current at room temperature and provides an adequate electron-hole pairs per absorbed photon. Moreover, the choice of materials with very high stopping powers makes the realization of thin detectors possible with resulting benefits in radiation tolerance and leakage currents. Unlike, materials characterized by very small stopping powers increase the detector scattering efficiency, which is a basic requirement for polarimetry measurements. A suitable choice of semiconductors having appropriate band gap and stopping power values, allows the fabrication of detectors with a very wide dynamic range.

However, compound semiconductors have some limitations such as poor mobility or reduced carrier lifetime of one or both charge carriers. Therefore, the mobility-lifetime product, which represents a classical detector

figure of merit, is for these materials lower than the corresponding value of the elemental semiconductors. The reason can be attribute to trapping centers caused by impurities, lack of stoichiometry, plastic deformations due to mechanical damage during fabrication processes.

CONCLUSIONS

In this study the principles of radiation matter interaction are reviewed. Both directly and indirectly ionizing beams are taken into account and their effects on the hit materials are analyzed. In particular, radiation interaction in semiconductors is studied and the behaviour of the classical p-n junction as detector is highlighted.

Moreover, a classification of the existing semiconductor detectors is indicated in function of the adopted material and the method by which the material is treated.

For the detector performance evaluation both some characteristic parameters and different operating modes are presented.

REFERENCES

Ahmed, S.N., 2007. Physics and Engineering of Radiation Detection. 1st Edn., Academic Press, Boston, ISBN-10: 0120455811, pp: 820.

Akimov, Y.K., 2007. Silicon radiation detectors (review). Instrum. Exp. Techn., 50: 1-28.

Beaumont, S.P., R. Bertin, C.N. Booth, C. Buttar and L. Carraresi *et al*., 1992. GaAs solid state detectors for particle physics. Nuclear Instrum. Meth. Phys. Res., 322: 472-482.

Bertolini, G. and A. Coche, 1968. Semiconductor Detectors. Elsevier Science, North-Holland Pub. Co., New York, ISBN-10: 044410142X, pp: 518.

Bertuccio, G., 2005. Prospect for energy resolving X-ray imaging with compound semiconductor pixel detectors. Nucl. Instrum. Meth. Phys. Res., 546: 232-241.

Cola, A., F. Quaranta, M. A. Ciocci and M. E. Fantacci, 1996. A study of the electrical and charge collection properties of semi-insulating GaAs detectors. Nucl. Instrum. Meth. Phys. Res., 380: 66-69.

Cola, A., F. Quaranta, L. Vasanelli, C. Canali, A. Cavallini, F. Nava and M.E. Fantacci, 1997. A study of the trap influence on the performances of semi-insulating GaAs pixel detectors. Nucl. Instrum. Meth. Phys. Res., 395: 349-354.

Dearnaley, G., 1966. Nuclear radiation detection by solid state devices. J. Sci. Instrum., 43: 869-869.

Dubari, E., H.E. Nilsson, C. Frojdh and B. Norlin, 2002. Monte carlo simulation of the response of a pixellated 3D photo-detector in silicon. Nucl. Instrum. Meth. Phys. Res., 487: 136-141.

Fano, U., 1947. Ionization yield of radiations II: The fluctuations of the number of ions. Phys. Rev., 72: 26-29.

Gibbons, P.E. and P. Iredale, 1967. On the accuracy of acceptor compensation by lithium ion drift. Nucl. Instrum. Meth., 53: 1-6.

Hoheisel, M., A. Korn and J. Giersch, 2005. Influence of backscattering on the spatial resolution of semiconductor X-ray detectors. Nucl. Instrum. Meth. Phys. Res. Sect. A: Accel. Spectromet. Detect. Assoc. Equip., 546: 252-257.

Jakubek, J., A. Cejnarovaa, T. Holya, S. Pospisila, J. Uhera and Z. Vykydal, 2008. Pixel detectors for imaging with heavy charged particles. Nucl. Instrum. Meth. Phys. Res. Sect. A: Accel. Spectromet. Detect. Assoc. Equip., 591: 155-158.

Janesick, J., T. Elliott and F. Pool, 1989. Radiation damage in scientific charge-coupled devices. IEEE Trans. Nucl. Sci., 36: 572-578.

Jevremovic, T., 2008. Nuclear Principles in Engineering. 2nd Edn., Springer-Verlag, Berlin, Heidelberg, ISBN-10: 0387856072.

Kim, S., H. Lee, C. Han, K. Lee and S. Choi *et al*., 1995. The effects of X-ray irradiation-induced damage on reliability in MOS structures. Solid-State Electron., 38: 95-99.

Knoll, G.F., 2010. Radiation Detection and Measurement. 4th Edn., John Wiley and Sons, New York, ISBN-10: 0470131489.

Lauber, A., 1969. The theory of compensation in lithium drifted semiconductor detectors. Nuclear Instruments Methods, 75: 297-308.

Leroy, C., P., Roy, G. Casse, M. Glaser, E. Grigoriev and F. Lemeilleur, 1999. Study of charge transport in non-irradiated and irradiated silicon detectors. Nucl. Instrum. Meth. Phys. Res. Sect. A: Accel. Spectromet. Detect. Assoc. Equip., 426: 99-108.

Leroy, C. and P.G. Rancoita, 2009. Principles of Radiation Interaction in Matter and Detection. 2nd Edn., World Scientific Publishing Co. SPte. Ltd., Singapore, ISBN: 978-981-281-827-0, pp: 950.

Lutz, G., 2007. Semiconductor Radiation Detectors: Device Physics. Springer, Berlin, Heidelberg, ISBN-10: 3540716785.

Millman, J. and A. Grabel, 1988. Microelectronics. 2nd Edn., McGraw-Hili, Singapore, ISBN-13: 978-0071005968.

Pell, E.M., 1960. Ion drift in an n-p junction. J. Applied Phys., 31: 291-302.

Ponpon, J.P., 2005. Semiconductor detectors for 2DX-ray imaging. Nucl. Instrum. Meth. Phys. Res., 551: 15-26.

Rizzi, M. and B. Castagnolo, 2003. Performance evaluation of X-Ray detector. WSEAS Trans. Circuits, 2: 70-75.

Rizzi, M., V. Antonicelli and B. Castagnolo, 2003. New model for a GaAs X-Ray pixel detector. IEE Proc. Circuits Devices Syst., 150: 210-216.

Rizzi, M., M. Maurantonio and B. Castagnolo, 2004. 3D-Finite element model for GaAs α-particles pixel detector. WSEAS Trans. Elect., 1: 595-600.

Rizzi, M., M. Maurantonio and B. Castagnolo, 2005. Novel microstrip system detectors for medical applications. WSEAS Trans. Biol. Biomed., 2: 220-227.

Rizzi, M., M. Maurantonio and B. Castagnolo, 2006a. Comparative analysis of GaAs, CdTe and CdZnTe radiation detectors. WSEAS Trans. Elect., 3: 7-13.

Rizzi, M., M. Maurantonio and B. Castagnolo, 2006b. GaAs X-Ray detector characterization through a 3D finite element model. J. Comput. Elect., 5: 27-34.

Tsoulfanidis, N., 1995. Measurement and Detection of Radiation. 2nd Edn., Taylor and Francis, London, ISBN-10: 1560323175, pp: 636.

Yaffe, M.J. and J.A. Rowlands, 1997. X-ray detectors for digital radiography. Phys. Med. Biol., 42: 1-39.